Chinese Journal of
POLYMER SCIENCE

RESEARCH ARTICLE

https://doi.org/10.1007/s10118-026-3637-2
Chinese J. Polym. Sci. **2026**, *44*, 2239–2247

Long Alkyl Tails Amplify Photoswitchable Glass Transition Temperatures of Azopolymers for Nanoimprint Lithography

Zhu-Lu Xie†, Fu-Wei Kong†, Jia-Hui Chen, Jie Yan, Bo-Ting Wang, Tian-Ren Zhao, Shuo-Feng Liang*, and Si Wu*

Hefei National Research Center for Physical Sciences at the Microscale, Anhui Key Laboratory of Optoelectronic Science and Technology, Department of Polymer Science and Engineering, University of Science and Technology of China, Hefei 230026, China

Electronic Supplementary Information

Abstract Azobenzene-containing polymers (azopolymers) exhibit photoinduced reversible solid-to-liquid transitions, enabling unique light-assisted nanoimprint lithography (NIL). *Cis* azopolymers possess sub-room-temperature glass transition temperatures (T_g), exhibiting liquid-like behavior for flow processing, while *trans* azopolymers feature above-room-temperature T_g values that enable solid-state shape fixation. Although many side-chain azopolymers demonstrate photoswitchable T_gs, conventional short-spacer derivatives show negligible switching in T_g as their *cis* isomers remain solid. This work overcomes this limitation in ethylene-spacer azopolymers through extended alkyl tails. We synthesized tailless (P0), *n*-butyl-tailed (P4), and *n*-decyl-tailed (P10) derivatives, revealing that only P10 exhibits a *cis* T_g near room temperature (22 °C) and an amplified ΔT_g between its *cis* isomer and *trans* isomer. P10 with photoswitchable T_gs enables complete nanostructure replication as a nanoimprint lithography photoresist. This work demonstrates that long alkyl tails counteract short-spacer limitations, effectively reducing the T_g of *cis* azopolymers and establishing a design principle for nanoimprint photoresists with photoswitchable T_gs.

Keywords Azobenzene; Photoresponsive polymers; Photoisomerization; Glass transition; Nanoimprint

Citation: Xie, Z. L.; Kong, F. W.; Chen, J. H.; Yan, J.; Wang, B. T.; Zhao, T. R.; Liang, S. F.; Wu, S. Long alkyl tails amplify photoswitchable glass transition temperatures of azopolymers for nanoimprint lithography. *Chinese J. Polym. Sci.* **2026**, *44*, 2239–2247.

INTRODUCTION

Glass transition temperature (T_g) is one of the most critical thermodynamic parameters for polymers, fundamentally governing their properties, processing, and applications.[1] The T_g and processing temperature jointly influence the processing behavior of polymers. Polymers exhibiting switchable T_gs at room temperature can simultaneously achieve processability and structural stability, making them suitable for advanced manufacturing processes, such as nanoimprint lithography (NIL). NIL is a technique that patterns nanostructures through mechanical deformation of a resist within a mold.[2] Current commercial NIL photoresists rely on UV curing and lack recyclability, while designing photoresists with switchable T_gs presents opportunities for reversible nanoimprint manufacturing.[3,4]

Recent studies have revealed that azobenzene-containing polymers (azopolymers) exhibit photoswitchable T_g values.[5,6] Reversible photoisomerization of azobenzene drives the photoinduced solid-to-liquid transitions in azobenzene-containing materials,[7–10] enabling applications in reversible adhesion,[11–14] healable materials,[15–18] solar energy storage,[19–22] and tunable mechanical properties.[23,24] Crucially, azopolymers permit room-temperature micro/nanoprocessing *via* light-assisted NIL.[3,25–27] *Cis* azopolymers (T_g < room temperature, liquid state) can fill molds under pressure or capillary force, whereas *trans* azopolymers (T_g > room temperature, solid state) can retain the replicated structures.[4] Molecular design strategies for azopolymers are essential for tuning their photoswitchable T_g, isomer-specific properties, and applications.

Side-chain azopolymers have been extensively studied for their unique properties, including liquid crystallinity,[28–32] self-assembly,[33–39] and directional photofluidization.[40–42] Molecular engineering of the backbone, spacer, azobenzene units, and tail groups enables reversible photoinduced solid-to-liquid transitions at room temperature in select systems.[43–45] Conventionally, only azopolymers bearing extended spacers, such as hexylene, display significant photoswitchable T_gs, making them suitable as photoresists for room-temperature NIL.[4,46] In contrast, azopolymers with short spacers (ethylene or none) exhibit no detectable photoswitchable T_gs, as their *cis* isomers remain solid with T_g values exceeding the temperature at which thermal reversion occurs.[43] Strategies to enhance ΔT_g between *trans* and *cis* azopolymers with short spacers through molecular design remain unexplored.

* Corresponding authors, E-mail: liangsf@ustc.edu.cn (S.F.L.)
E-mail: siwu@ustc.edu.cn (S.W.)
† These authors contributed equally to this work.
Received February 3, 2026; Accepted February 27, 2026; Published online June 3, 2026

In this study, we demonstrate how tail groups govern T_g switching in short-spacer azopolymers by synthesizing three ethylene-spacer derivatives: tailless (P0), n-butyl-tailed (P4), and *n*-decyl-tailed (P10). While all three exhibited reversible photoisomerization, only P10 possessed photoswitchable T_gs values, enabling faithful pattern replication *via* room-temperature photo-nanoimprinting. The extended alkyl tail critically depresses the T_g of *cis* isomer below its thermal reversion threshold and amplifies the ΔT_g between *cis* and *trans* isomers. This strategy counteracts the adverse effects of short spacers on the photoinduced solid-to-liquid transition and advances the design of azopolymer photoresists for room-temperature NIL.

EXPERIMENTAL

The synthetic details, experimental section, and complementary data are presented in the electronic supplementary information (ESI).

RESULTS AND DISCUSSION

Three ethylene spacer azopolymers (tailless P0, *n*-butyl tailed P4, and *n*-decyl-tailed P10) were synthesized *via* RAFT polymerization (Fig. 1a). The ^{1}H nuclear magnetic resonance (^{1}H-NMR) spectra of azobenzene-containing monomers M0, M4, M10 and azopolymers P0, P4, P10 (Figs. 1b and 1c) revealed post-polymerization peak broadening and complete disappearance of the methacrylate proton signal at 5.5–6.3 ppm, confirming successful polymerization. Gel permeation chromatography (GPC) analysis indicated that the number-average molecular weights of P0, P4, and P10 were 11, 11, and 20 kg·mol^{-1}, respectively (Fig. S7 in ESI).

All three azopolymers underwent reversible photoisomerization (Fig. 2a, Fig. S8 in ESI). UV-Vis spectra of spin-coated films of azopolymers showed strong π-π^* transitions at about 340 nm and weaker n-π^* bands at about 450 nm (Figs. 2b–2d). UV irradiation (365 nm, 4.1 mW·cm^{-2}) decreased the π-π^* intensity and increased the n–π^* absorption, indicating *trans*-to-*cis* isomerization. Subsequent visible light exposure (530 nm, 5.2 mW·cm^{-2}) reversed these changes *via* *cis*-to-*trans* isomerization. Azobenzene groups can form H-aggregates, free chromophores, and J-aggregates in the solidstate. Gaussian fitting of the pre-irradiation spectra of the azopolymers identified three peaks corresponding to H-aggregates, free azobenzene, and J-aggregates (Fig. S9 in ESI),[47,48] with P0 exhibiting the highest free azobenzene content. Although Gaussian fitting is not quantitative, it reliably indicates the relative aggregate proportions. After visible light irradiation, the spectra of the azopolymers differed from the initial states because of the significantly reduced azobenzene aggregation after alternating UV and visible light exposure. The initial films were obtained through annealing, and the aggregation state of the azobenzene chromophores in this state critically depended on the thermal history. All three films were cycled between *trans* and *cis* states five times by alternating UV and visible light irradiation (Figs. 2e–2g), exhibiting reversible photoisomerization between photostationary states under 365 nm and 530 nm irradiation.

Next, we investigated the photoinduced solid-to-liquid transition behavior of the three azopolymers. Microscopic observations of the azopolymer powders under UV irradiation revealed distinct morphological changes (Fig. 3). While P0 and P4 powders showed no significant alterations, the P10 powder exhibited progressive edge rounding that culminated in droplet formation over the irradiation time.

Thermogravimetric analysis (TGA) confirmed comparable decomposition temperatures for P0, P4, and P10 (Fig. S10 in ESI). The thermal behaviors of *trans* and *cis* azopolymers were investigated using differential scanning calorimetry (DSC) (Fig. 4). Before the DSC testing, the samples were dried in a vacuum oven at 40 °C for 12 h. The first heating process rep-

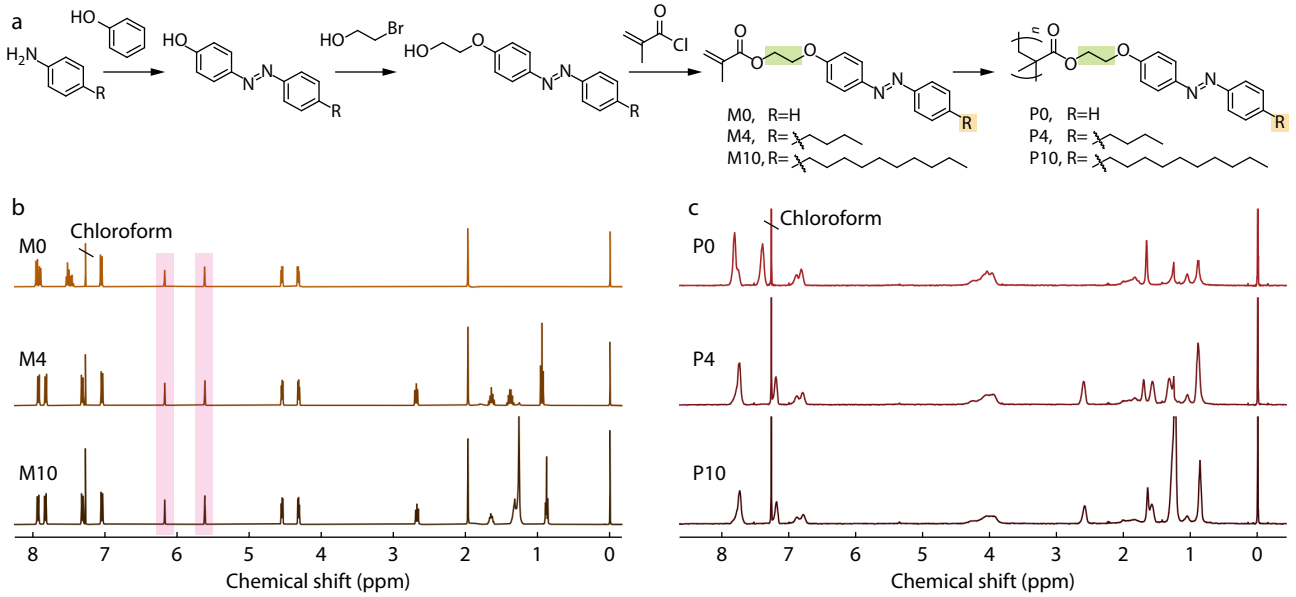

Fig. 1 (a) Synthetic routes of P0, P4, and P10; (b) ^{1}H-NMR spectra of azobenzene-containing monomers M0, M4, and M10; (c) ^{1}H-NMR spectra of azopolymers P0, P4, and P10.

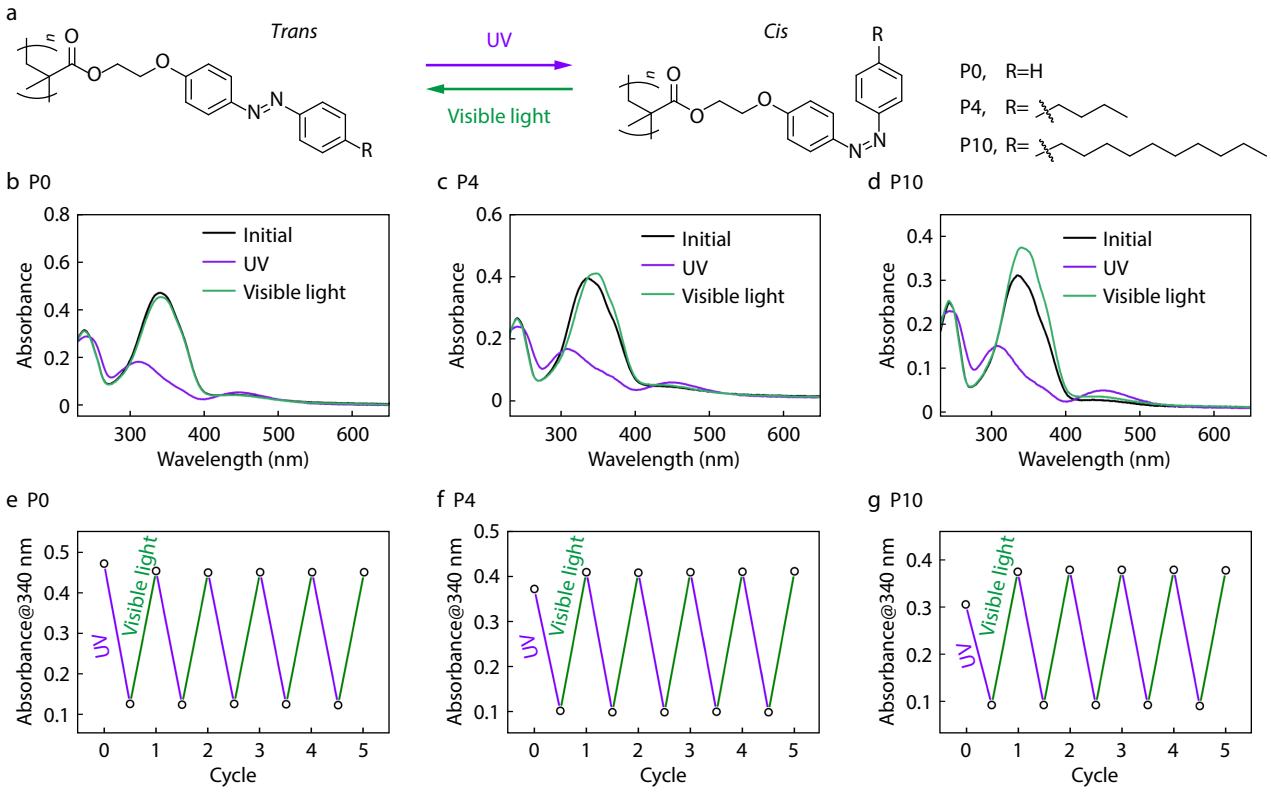

Fig. 2 (a) Photoisomerization of azopolymers P0, P4, and P10; (b–d) UV-Vis absorption spectra of spin-coated films of P0 (b), P4 (c), and P10 (d) at initial state, after UV irradiation (365 nm, 4.1 mW·cm^{-2}, P0: 1 min; P4, P10: 2 min) and subsequent visible light irradiation (530 nm, 5.2 mW·cm^{-2}, P0: 8 min; P4, P10: 3 min). (e–g) Changes in the absorption maxima of P0 (e), P4 (f), and P10 (g) films under alternating UV and visible light irradiation.

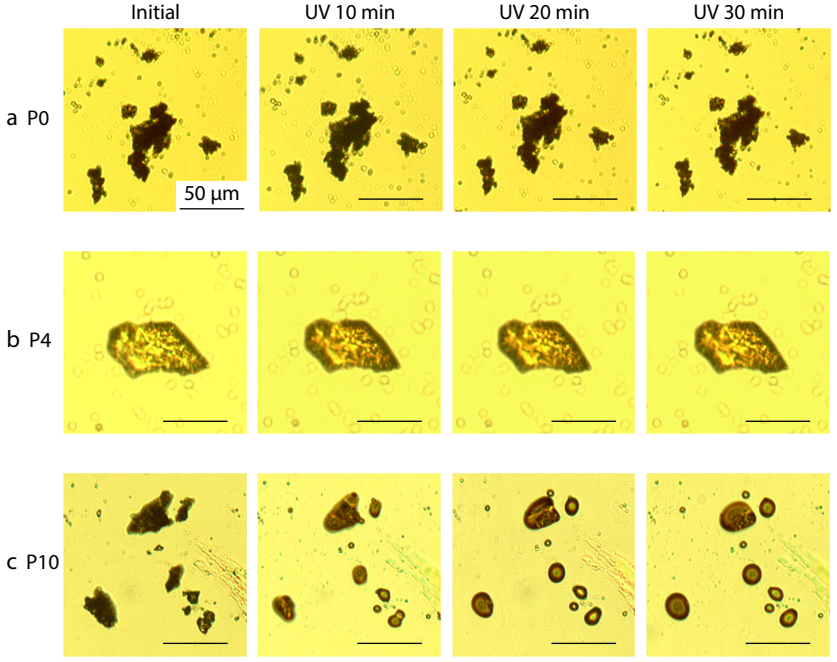

Fig. 3 Optical microscopy images of powders of P0 (a), P4 (b) and P10 (c) before and after UV irradiation (365 nm, 24.1 mW·cm^{-2}) for 10, 20, and 30 min at 30 °C.

resented the thermal history of the samples. The second heating scan of *trans* azopolymers revealed T_g values of 62 °C for P0 and 118 °C for P10, but no discernible T_g was observed for P4 (Figs. 4a–4c). Clearing points emerged at 145 and 183 °C for P4 and P10, respectively, whereas P0 exhibited neither a clearing point nor mesophase. The clearing points measured

by DSC were consistent with the polarized optical microscopy observations (Fig. S11 in ESI). In addition, P4 and P10 exhibit photoinduced phase transitions (Fig. S12 in ESI).

For *cis* azopolymers, all three samples displayed broad exothermic peaks near 50 °C during the first heating cycle, corresponding to *cis*-to-*trans* thermal relaxation and the subsequent reorganization of *trans* azobenzene aggregates (Figs. 4d–4f).[20,49] Critically, no T_g was observed for any *cis* azopolymer prior to thermal relaxation. The second heating curves of *cis* samples were aligned with those of *trans* samples after thermal reversal to the *trans* state.

Owing to the inconspicuous glass transitions in some DSC profiles, rheological analyses were employed to characterize *trans* and *cis* azopolymers. Temperature-dependent rheological tests revealed T_g values of *trans* P0, P4, and P10 were 85, 127, and 114 °C, respectively (Figs. 5a–5c) based on the decline in storage moduli (*G*′). All *trans* azopolymers exhibited T_g values above room temperature, confirming their solid state at room temperature. In the rheological tests, *G*′ and *G*″ are relative values, because some of the samples lost contact with the sample plates. The use of relative values did not influence the loss tangent (tan*δ*). Frequency sweep tests fur-

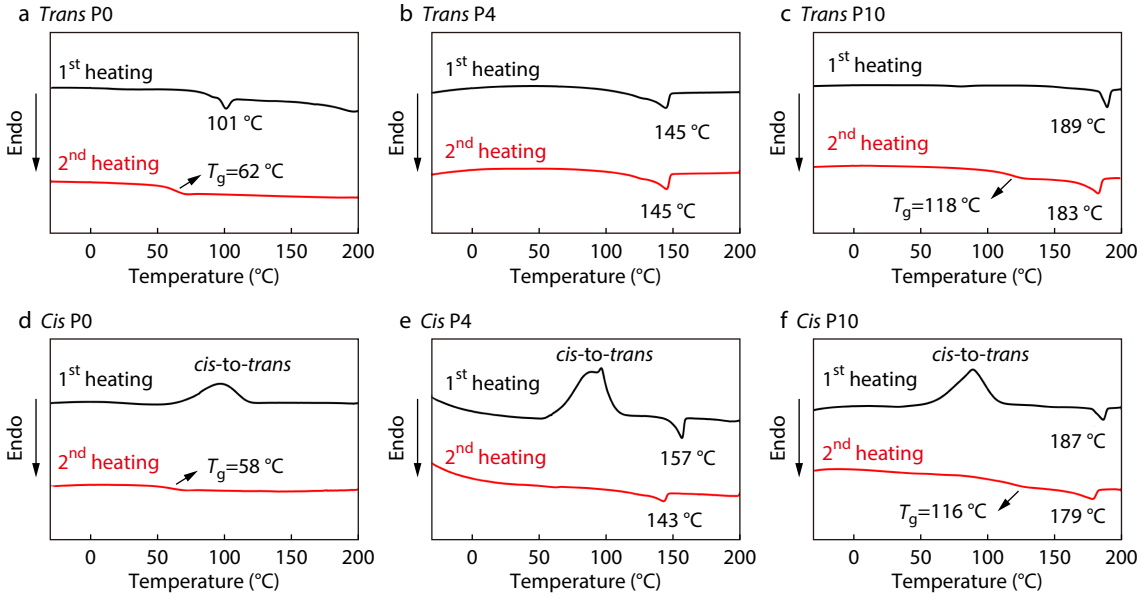

Fig. 4 (a–c) First and second heating DSC curves of *trans* P0 (a), P4 (b), and P10 (c); (d–f) First and second heating DSC curves of *cis* P0 (d), P4 (e), and P10 (f) (scan rate: 10 °C·min^{-1}). The *cis* contents of *cis* P0, P4, and P10 were 87%, 88%, and 90%, respectively (Figs. S13–S15 in ESI).

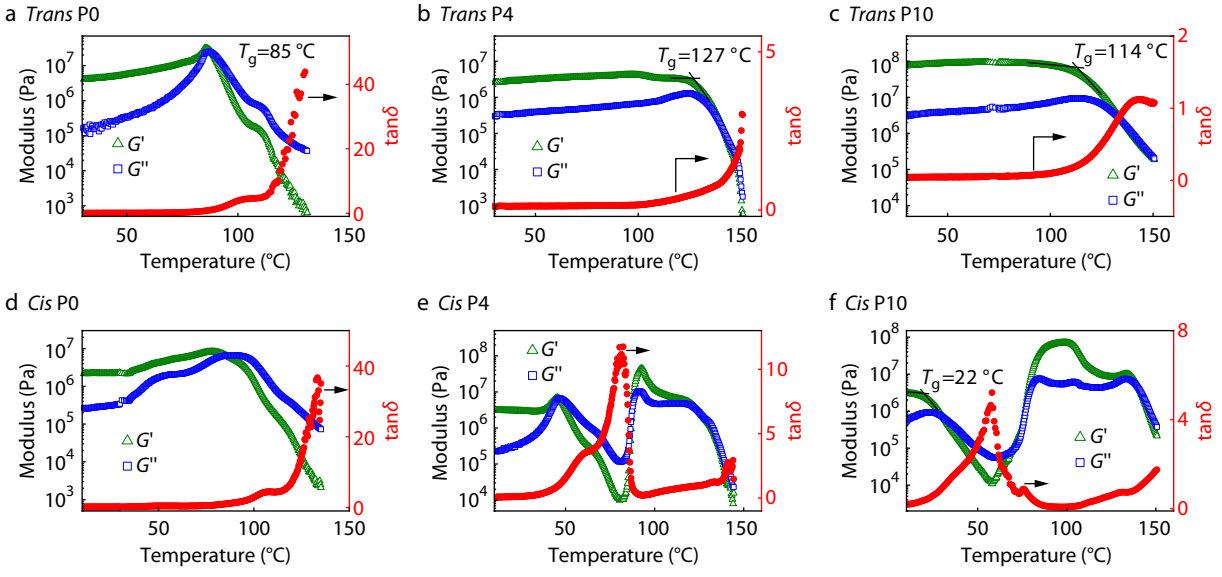

Fig. 5 (a–c) Temperature-dependent rheological profiles of *trans* P0 (a), P4 (b), and P10 (c); (d–f) Temperature-dependent rheological profiles of *cis* P0 (d), P4 (e), and P10 (f) (heating rate: 3 °C·min^{-1}). The *cis* contents of *cis* P0, P4, and P10 were 87%, 88%, and 90%, respectively (Figs. S13–S15 in ESI). *G*′: storage modulus; *G*″: loss modulus; tan*δ* = *G*″/*G*′: loss tangent. *G*′ and *G*″ are relative values because part of the samples lost contact with the sample plates. The use of the relative values did not influence tan*δ*.

https://doi.org/10.1007/s10118-026-3637-2

ther validated the solid-like behaviors, with the storage moduli (G') of *trans* azopolymers consistently exceeding their loss moduli (G'') across the measured angular frequency range (Fig. S16 in ESI)

For *cis* P0 and *cis* P4, G' remained greater than G'' below 40 °C with no detectable T_g (Figs. 5d and 5e). Above 40 °C, *cis* P0 underwent thermal reversion to *trans* P0 while exhibiting a gradual modulus increase. In contrast, *cis* P4 exhibited $G' < G''$ beyond 40 °C, likely owing to the concurrent glass transition and thermal reversion of *cis* P4. Critically, *cis* P0 and *cis* P4 displayed no glass transition prior to the thermal reversion threshold (< 40 °C) and maintained a solid character at room temperature, corroborated by the frequency sweep results (Fig. S16 in ESI). Among *cis* azopolymers, only *cis* P10 exhibited a discernible T_g of 22 °C before thermal reversion (Fig. 5f). Frequency sweeps of *cis* P10 showed liquid-like behavior ($G' < G''$) at low frequencies and solid-like response ($G' > G''$) at high frequencies, indicating non-Newtonian fluid characteristics at room temperature (Fig. S16 in ESI). As a result, P10 is the sole system that demonstrates a photoswitchable T_gs. The *trans* T_g, *cis* T_g, and ΔT_g values of the three azopolymers are summarized in Table 1. The ΔT_g values for P0, P4, and P10 were < 45 °C, < 87 °C, and 92 °C, respectively. Rheological evidence confirms that extended tail groups enable *cis* azopolymers with short spacers to undergo glass transition before thermal reversion and enhance the ΔT_g.

Atomic force microscopy (AFM) force curve analysis further elucidated the interfacial properties of *trans* and *cis* azopolymers (Fig. 6). Thin films of all the three azopolymers were prepared by drop casting. UV irradiation converted the film surface into a *cis*-rich state. The dipole moment difference between *trans* and *cis* azobenzenes alters the surface energy of the azopolymers. The contact angle measurements confirmed the formation of *cis*-rich surfaces (Fig. S17 in ESI). Both isomers of P0 exhibited identical adhesion forces and displacements (Figs. 6a and 6d). The approach curves showed linear force-distance relationships, while the retraction curves revealed adhesion dominated by van der Waals forces, consistent with solid-like surfaces. In contrast, *cis* P4 demonstrated a moderately higher adhesion than *trans* P4, indicating surface softening after UV irradiation (Figs. 6b and 6e). Crucially, *trans* P10 exhibited a characteristic hard-surface behavior, whereas *cis* P10 displayed significantly enhanced adhesion to the tip during retraction (Figs. 6c and 6f). This manifested as liquid-like characteristics, where viscous *cis*-rich P10 formed menisci at the AFM tip.

Photoswitchable T_gs enable reversible transitions between a processable liquid-like state and a moldable solid state in azopolymers. This room-temperature photoprocessability permits their use as NIL photoresists (Fig. 7a). We evaluated three azopolymers as NIL resists by spin-coating thin films, pressing a striped-nanostructure PDMS mold onto the films, UV irradiation to generate *cis*-rich surfaces, and applying visible light to revert *cis* azopolymers to *trans* states before demolding. The AFM analysis revealed distinct replication patterns. P0 exhibited negligible microstructure formation (Fig. 7b). P4 exhibited fragmented striped patterns, indicating partial softening after UV irradiation under pressure aligned with its force curve behavior (Fig. 7c). P10 achieved a complete replica of the nanostructures of the PDMS mold, demonstrating that its low T_g in the *cis* state enhanced fluidity and processability. Photoswitchable T_gs enables P10 to function as an effective NIL resist (Fig. 7d). The nanoimprinted P10 polymer

Table 1 *Trans* T_g, *cis* T_g, and ΔT_g values of three azopolymers. [a]

Azopolymer	*Trans* T_g (°C)	*Cis* T_g (°C)	ΔT_g (°C)
P0	85	> 40	< 45
P4	127	> 40	< 87
P10	114	22	92

[a]The T_g values were determinded by rheological tests.

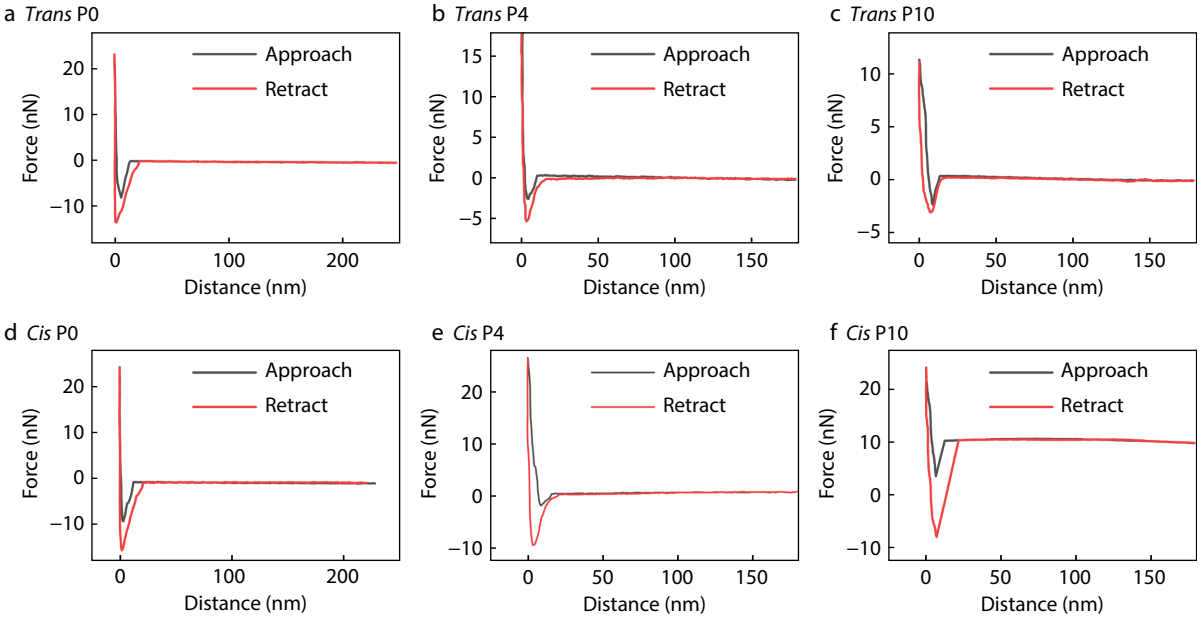

Fig. 6 AFM force-distance curves of *trans* P0 (a), P4 (b), and P10 (c) films and *cis* P0 (d), P4 (e), and P10 (f) films. The *cis* films were prepared by irradiating *trans* films with UV light (365 nm, 10.4 mW·cm^{-2}, 1 min).

https://doi.org/10.1007/s10118-026-3637-2

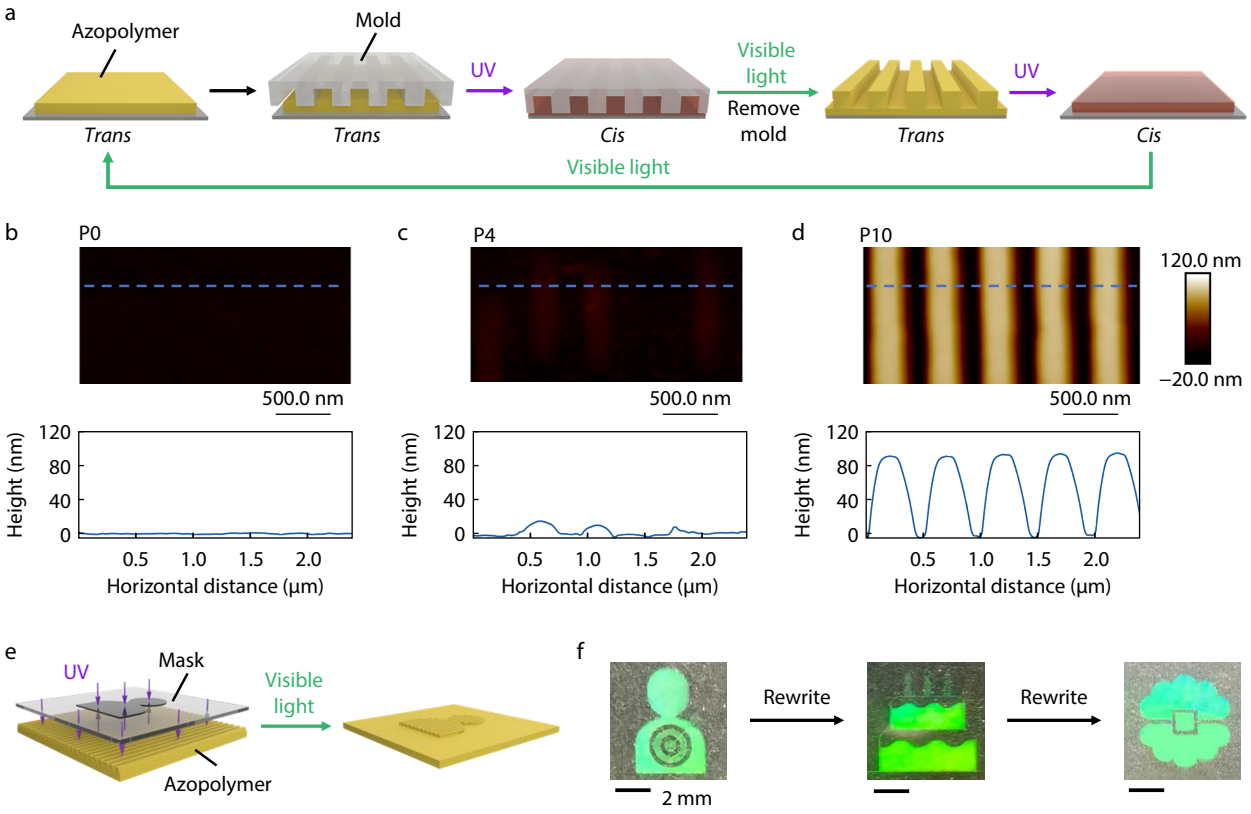

Fig. 7 (a) Schematic illustration of the light-assisted nanoimprinting process. UV: 365 nm, 10.4 mW·cm^{-2}, 5 min. Visible light: 530 nm, 17.3 mW·cm^{-2}, 5 min. (b–d) Atomic force microscopy (AFM) images and the corresponding cross-sectional height profiles of P0 (b), P4 (c), and P10 (d). (e) Schematic illustration of the fabrication of photonic crystal patterns by photomask-assisted irradiation. UV irradiation: 365 nm, 10.4 mW·cm^{-2}, 2 min. Visible light irradiation: 530 nm, 17.3 mW·cm^{-2}, 2 min. (f) Photonic crystal patterns fabricated from P10. The photonic crystal patterns can be erased by UV irradiation (365 nm, 10.4 mW·cm^{-2}, 2 min). After another cycle of light-assisted nanoimprinting and photomask-assisted irradiation, the pattern can be rewritten.

films enabled region-specific patterning *via* UV irradiation (Fig. 7e). UV exposure through a photomask selectively liquefied the regions in the imprinted P10 film, causing localized nanostructure collapse to generate a photonic crystal pattern (Fig. 7f). Cyclic UV erasure and re-imprinting enabled the P10 pattern reconstruction, confirming the capability of P10 as a reversible NIL photoresist.

CONCLUSIONS

This work resolves the critical limitation of conventional short-spacer azopolymers in achieving photoswitchable T_gs by introducing a molecular design strategy based on extended alkyl tails. Through systematic synthesis and characterization of ethylene-spacer azobenzene derivatives (P0, P4, and P10), we demonstrated that *n*-decyl tailing induces a reduction in *cis* T_g to near-room-temperature conditions (22 °C) and amplifies the ΔT_g value. However, *cis* glass transitions were not attainable before the thermal reversion threshold in tailless or short-tailed analogs. P10 exhibited solid-state behavior in *trans* configuration while displaying non-Newtonian fluid characteristics in its *cis* state, enabling its application as an NIL resist. This molecular design principle fundamentally addresses the constraints of short-spacer azopolymers, establishing tail-engineered derivatives as enabling materials for ambient-temperature nanofabrication processes.

Conflict of Interests

The authors declare no interest conflict.

Electronic Supplementary Information

Electronic supplementary information (ESI) is available free of charge in the online version of this article at http://doi.org/10.1007/s10118-026-3637-2.

Data Availability Statement

The data supporting the findings of this study are available from the corresponding authors upon reasonable request.

ACKNOWLEDGMENTS

This work was financially supported by the National Natural Science Foundation of China (Nos. 52503162, 52425302, 52120105004, and 52350233), Hefei Municipal Natural Science Foundation (No. HZR2518), Fundamental Research Funds for

the Central Universities (Nos. WK3450000006 and WK2060190102), Anhui Provincial Natural Science Foundation (Nos. 1908085MB38 and 2508085QB046), and Postdoctoral Fellowship Program of CPSF (No. GZB20250013). This work was partially carried out at the USTC Center for Micro and Nanoscale Research and Fabrication and the Instruments Center for Physical Science, University of Science and Technology of China.

REFERENCES

1 Napolitano, S.; Glynos, E.; Tito, N. B. Glass transition of polymers in bulk, confined geometries, and near interfaces. *Rep. Prog. Phys.* **2017**, *80*, 036602.
2 Traub, M. C.; Longsine, W.; Truskett, V. N. Advances in nanoimprint lithography. *Annu. Rev. Chem. Biomol. Eng.* **2016**, *7*, 583–604.
3 Liang, S.; Yuan, C.; Nie, C.; Liu, Y.; Zhang, D.; Xu, W.-C.; Liu, C.; Xu, G.; Wu, S. Photocontrolled reversible solid-fluid transitions of azopolymer nanocomposites for intelligent nanomaterials. *Adv. Mater.* **2024**, *36*, e2408159.
4 Xu, W.-C.; Liu, C.; Liang, S.; Zhang, D.; Liu, Y.; Wu, S. Designing rewritable dual-mode patterns using a stretchable photoresponsive polymer *via* orthogonal photopatterning. *Adv. Mater.* **2022**, *34*, 2202150.
5 Zhou, H.; Xue, C.; Weis, P.; Suzuki, Y.; Huang, S.; Koynov, K.; Auernhammer, G. K.; Berger, R.; Butt, H. J.; Wu, S. Photoswitching of glass transition temperatures of azobenzene-containing polymers induces reversible solid-to-liquid transitions. *Nat. Chem.* **2017**, *9*, 145–151.
6 Xu, W. C.; Sun, S.; Wu, S. Photoinduced reversible solid-to-liquid transitions for photoswitchable materials. *Angew. Chem. Int. Ed.* **2019**, *58*, 9712–9740.
7 Bandara, H. M. D.; Burdette, S. C. Photoisomerization in different classes of azobenzene. *Chem. Soc. Rev.* **2012**, *41*, 1809–1825.
8 Jerca, F. A.; Jerca, V. V.; Hoogenboom, R. Advances and opportunities in the exciting world of azobenzenes. *Nat. Rev. Chem.* **2021**, *6*, 51–69.
9 Dang, T.; Zhang, Z.-Y.; Li, T. Visible-light-activated heteroaryl azoswitches: toward a more colorful future. *J. Am. Chem. Soc.* **2024**, *146*, 19609–19620.
10 Liang, S.; Yuan, C.; Wang, M.; Wu, S. Photoresponsive polymer nanocomposites: dynamic materials with photocontrolled functions. *CCS Chem.* **2025**, *7*, 2950–2969.
11 Yue, Y.; Norikane, Y.; Nishibori, E. Biomimetic adhesion/detachment using layered polymers with light-induced rapid shape changes. *Angew. Chem. Int. Ed.* **2025**, *64*, e202503748.
12 Lin, Z.; Feng, J.; Fang, L.; Zhang, Y.; Ran, Q.; Zhu, Q.; Yu, D. Transforming commercial polymers into tough yet switchable adhesives by trident photoswitch molecule doping: break

Graphical Abstract

Long Alkyl Tails Amplify Photoswitchable Glass Transition Temperatures of Azopolymers for Nanoimprint Lithography

Zhu-Lu Xie, Fu-Wei Kong, Jia-Hui Chen, Jie Yan, Bo-Ting Wang, Tian-Ren Zhao, Shuo-Feng Liang, and Si Wu

University of Science and Technology of China

Azobenzene-containing polymers exhibit photoswitchable glass-transition temperatures when modified with long alkyl tails. This tail-engineering approach fundamentally overcomes the spacer length limitations and establishes a generalizable design principle for reversible nanoimprint photoresists.

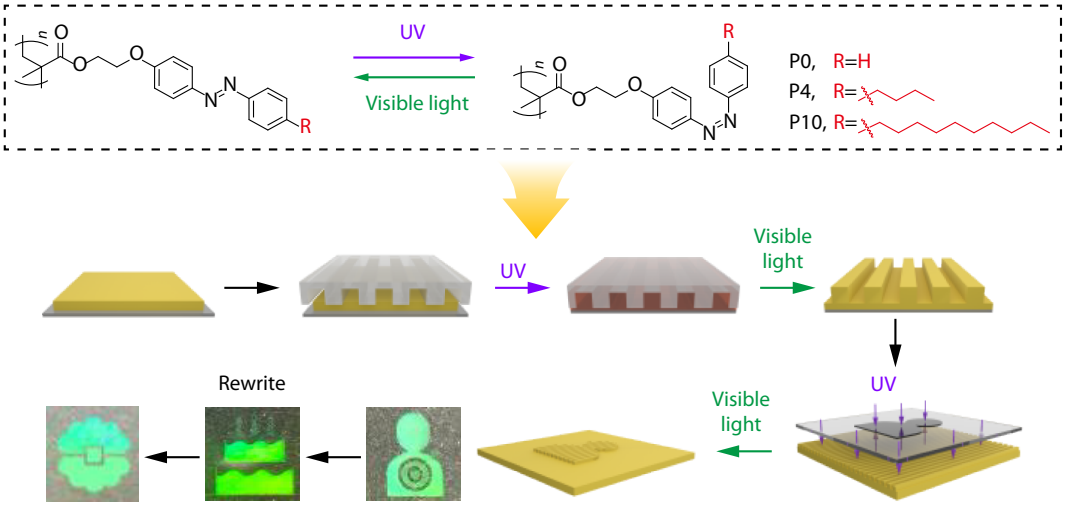

Chinese J. Polym. Sci. 2026, 44, 2239–2247 *https://doi.org/10.1007/s10118-026-3637-2*

adhesion-switchability paradox. *Adv. Mater.* **2024**, *36*, e2406459.
13 Zhao, R.; Mu, J.; Bai, J.; Zhao, W.; Gong, P.; Chen, L.; Zhang, N.; Shang, X.; Liu, F.; Yan, S. Smart responsive azo-copolymer with photoliquefaction for switchable adhesive application. *ACS Appl. Mater. Interfaces* **2022**, *14*, 16678–16686.
14 Shen, D.; Yao, Y.; Zhuang, Q.; Lin, S. Mainchain alternating azopolymers with fast photo-induced reversible transition behavior. *Macromolecules* **2021**, *54*, 10040–10048.
15 Zhou, J.; Zhou, N.; Xu, W.; Qian, Z.; Dai, Z.; Xu, J.; Chen, J.; Xiong, Y. Photo-tuned solid-liquid transition of azo-grafted poly(thioctic acid) with ultrahigh photothermal conversion efficiency. *Angew. Chem. Int. Ed.* **2025**, *64*, e202508314.
16 Hsu, Y. S.; Tsai, T. H.; Chang, C. C.; Lo, T. Y.; Kuo, K. C.; Lin, Y. C.; Lin, J.; Manibalan, K.; Chang, C. W.; Ho, J. H.; Lin, C. T.; Chen, J. T. Photo-healable and stretchable fibers from upcycled tpee and azopolymers by harnessing solid-to-liquid photoisomerization. *ACS Appl. Mater. Interfaces* **2025**, *17*, 51256–51266.
17 Chen, M.; Yao, B.; Kappl, M.; Liu, S.; Yuan, J.; Berger, R.; Zhang, F.; Butt, H.-J.; Liu, Y.; Wu, S. Entangled azobenzene-containing polymers with photoinduced reversible solid-to-liquid transitions for healable and reprocessable photoactuators. *Adv. Funct. Mater.* **2019**, *30*, 201906752.
18 Liu, Y.; Liang, S.; Yuan, C.; Best, A.; Kappl, M.; Koynov, K.; Butt, H.-J.; Wu, S. Fabrication of anticounterfeiting nanocomposites with multiple security features *via* integration of a photoresponsive polymer and upconverting nanoparticles. *Adv. Funct. Mater.* **2021**, *31*, 2103908.
19 Xu, X.; Li, C.; Chen, W.; Feng, J.; Li, W.-Y.; Wang, G.; Yu, H. Visible light activated dendrimers for solar thermal energy storage and release below 0 °C. *J. Mater. Chem. A* **2024**, *12*, 23723–23731.
20 Cai, F.; Song, T.; Yang, B.; Lv, X.; Zhang, L.; Yu, H. Enhancement of solar thermal fuel by microphase separation and nanoconfinement of a block copolymer. *Chem. Mater.* **2021**, *33*, 9750–9759.
21 Zhang, Z.-Y.; He, Y.; Wang, Z.; Xu, J.; Xie, M.; Tao, P.; Ji, D.; Moth-Poulsen, K.; Li, T. Photochemical phase transitions enable coharvesting of photon energy and ambient heat for energetic molecular solar thermal batteries that upgrade thermal energy. *J. Am. Chem. Soc.* **2020**, *142*, 12256–12264.
22 Han, G. G. D.; Li, H.; Grossman, J. C. Optically-controlled long-term storage and release of thermal energy in phase-change materials. *Nat. Commun.* **2017**, *8*, 1446.
23 Chen, C.; Ji, Y.; Li, H.; Song, T.; Yu, H. Unusual photo-tunable mechanical transformation of azobenzene terminated aliphatic polycarbonate. *Nat. Commun.* **2025**, *16*, 2620.
24 Cai, F.; Yang, B.; Lv, X.; Feng, W.; Yu, H. Mechanically mutable polymer enabled by light. *Sci. Adv.* **2022**, *8*, eabo1626.
25 Ji, Y.; Song, T.; Yu, H. Assembly-induced dynamic structural color in a host-guest system for time-dependent anticounterfeiting and double-lock encryption. *Angew. Chem. Int. Ed.* **2024**, *63*, e202401208.
26 Pan, F.; Feng, Y.; Qian, Y.; Qin, L.; Yu, Y. Dual-mode patterns enabled by photofluidization of an azobenzene-containing linear liquid crystal copolymer. *Langmuir* **2024**, *40*, 11766–11774.
27 Yuan, C.; Zhang, D.; Xie, Z.; Xu, W.-C.; Liang, S.; Wu, S. Heterogeneous polymer multilayers enabling photoresponsive nonreciprocal patterns for information encryption. *Adv. Mater.* **2025**, *37*, e2506950.
28 Ji, B.; Qin, L.; Yu, Y. L. Dynamic structural colors in helical superstructures: from supramolecules to polymers. *Chinese J. Polym. Sci.* **2025**, *43*, 406–428.
29 Lugger, S. J. D.; Ceamanos, L.; Mulder, D. J.; Sánchez-Somolinos, C.; Schenning, A. P. H. J. 4D printing of supramolecular liquid crystal elastomer actuators fueled by light. *Adv. Mater. Technol.* **2022,** *8*, 2201472.
30 Zhao, X.; Chen, Y.; Peng, B.; Wei, J.; Yu, Y. A facile strategy for the development of recyclable multifunctional liquid crystal polymers *via* post-polymerization modification and ring-opening metathesis polymerization. *Angew. Chem. Int. Ed.* **2023**, *62*, e202300699.
31 Guo, H.; Nasare, R.; Liang, C.; Kuntze, K.; Terentjev, E. M.; Priimagi, A. Halogen-bonded liquid crystal elastomers as initiator-free photochemical actuators. *Adv. Mater.* **2025**, *37*, e2504551.
32 Qu, G.; Zhang, X.; Li, S.; Lu, L.; Gao, J.; Yu, B.; Wu, S.; Zhang, Q.; Hu, Z. Liquid crystal random lasers. *Phys. Chem. Chem. Phys.* **2022**, *25*, 48–63.
33 Gao, M. D.; Guan, C. Y.; Wang, J. Y.; Qi, J. Y.; Deng, N. N. Thermally switchable photoactivity in azobenzene-functionalized dna condensates. *Adv. Mater.* **2025,** e18318.
34 Li, H. T.; Zhang, W. L.; He, Y. N. Non-covalently functionalized carbon nanotube by hyaluronic acid based azo polymer for photothermal elimination of tumor cells. *Chinese J. Polym. Sci.* **2025**, *43*, 1785–1791.
35 Sun, Z.; Xu, Z.; Ding, M.; Wang, L.; Zhao, L.; Sui, P.; Li, G.; Jin, H.; Zhou, Y.; Lin, S. Ultrathin polymersomes with controllable light-responsivity *via* adjusting the electronic effect from para-substituents of azobenzene. *Angew. Chem. Int. Ed.* **2025**, *64*, e202503104.
36 Zhao, Q. H.; Qi, J. Y.; Deng, N. N. DNA photofluids show life-like motion. *Nat. Mater.* **2025**, *24*, 935–944.
37 Liu, C.; Yang, Z.; Song, X.; Qian, Y.; Huo, H.; He, J.; Zhang, J.; Zhang, Z.; Shi, M.; Pang, J.; Zhang, B.; Tian, W. Light controlled drug-based supramolecular polymer self-assemblies for efficient antibacterial manipulation. *Supramol. Mater.* **2022**, *1*, 100014.
38 Ma, W.; Wang, B.; Wang, D.; Liu, Y.; Jiang, M.-C.; Zhang, J.-Y.; Peng, D.-D.; Li, Z.-C.; Yu, C.-Y.; Wei, H. A self-cascade terpolymer platform for amplified chemo-chemodynamic therapy with synergistic immunogenic cell death enhancement. *Supramol. Mater.* **2024**, *3*, 100066.
39 Cheng, X.; Miao, T.; Zhang, G.; Guo, J.; Zhou, Z.; Zhang, W. Switchable Phase Helicity Independent of the Absolute Configuration of the Stereocenter: anomalous induction between sergeants and soldiers in chiral liquid-crystalline polymers. *J. Am. Chem. Soc.* **2023**, *145*, 16474–16487.
40 Lee, S.; Kang, H. S.; Park, J. K. Directional photofluidization lithography: micro/nanostructural evolution by photofluidic motions of azobenzene materials. *Adv. Mater.* **2012**, *24*, 2069–2103.
41 Kang, H. S.; Jolly, J. C.; Cho, H.; Kalpattu, A.; Zhang, X. A.; Yang, S. Three-Dimensional Photoengraving of Monolithic, Multifaceted Metasurfaces. *Adv. Mater.* **2020**, *33*, 202005454.
42 Liang, S. F.; Nie, C.; Yan, J.; Zhang, Q. J.; Wu, S. Photoinduced reversible solid-to-liquid transitions and directional photofluidization of azobenzene-containing polymers. *Chinese J. Polym. Sci.* **2020**, *39*, 1225–1234.
43 Weis, P.; Hess, A.; Kircher, G.; Huang, S.; Auernhammer, G. K.; Koynov, K.; Butt, H.-J.; Wu, S. Effects of spacers on photoinduced reversible solid-to-liquid transitions of azobenzene-containing polymers. *Chem. - Eur. J.* **2019**, *25*, 10946–10953.
44 Zhang, Z.; Chen, M.; Schneider, I.; Liu, Y.; Liang, S.; Sun, S.; Koynov, K.; Butt, H.-J.; Wu, S. Long alkyl side chains simultaneously improve mechanical robustness and healing ability of a photoswitchable polymer. *Macromolecules* **2020**, *53*, 8562–8569.
45 Liang, S.; Li, S.; Yuan, C.; Zhang, D.; Chen, J.; Wu, S. Polyacrylate backbone promotes photoinduced reversible solid-to-liquid transitions of azobenzene-containing polymers. *Macromolecules* **2023**, *56*, 448–456.
46 Liu, C.; Steppert, A. K.; Liu, Y.; Weis, P.; Hu, J.; Nie, C.; Xu, W.-C.; Kuehne, A. J. C.; Wu, S. A Photopatternable conjugated polymer with thermal-annealing-promoted interchain stacking for highly

stable anti-counterfeiting materials. *Adv. Mater.* **2023**, *35*, 202303120.
47 Menzel, H.; Weichart, B.; Schmidt, A.; Paul, S.; Knoll, W.; Stumpe, J.; Fischer, T. Small-angle X-ray scattering and ultraviolet-visible spectroscopy studies on the structure and structural changes in langmuir-blodgett films of polyglutamates with azobenzene moieties tethered by alkyl spacers of different length. *Langmuir* **2002**, *10*, 1926–1933.
48 Tong, X.; Cui, L.; Zhao, Y. Confinement effects on photoalignment, photochemical phase transition, and thermochromic behavior of liquid crystalline azobenzene-containing diblock copolymers. *Macromolecules* **2004**, *37*, 3101–3112.
49 Ishiba, K.; Morikawa, M. A.; Chikara, C.; Yamada, T.; Iwase, K.; Kawakita, M.; Kimizuka, N. Photoliquefiable ionic crystals: a phase crossover approach for photon energy storage materials with functional multiplicity. *Angew. Chem. Int. Ed.* **2014**, *54*, 1532–1536.

https://doi.org/10.1007/s10118-026-3637-2